ARTICLE

BIOTECHNOLOGY and BIOENGINEERING

More Similar Than Different: Host Cell Protein Production Using Three Null CHO Cell Lines

Inn H. Yuk,[1] Julie Nishihara,[2] Donald Walker Jr,[2] Eric Huang,[1] Feny Gunawan,[3] Jayashree Subramanian,[1] Abigail F.J. Pynn,[1] X.Christopher Yu,[2] Judith Zhu-Shimoni,[2] Martin Vanderlaan,[3] Denise C. Krawitz[3]

[1]Early Stage Cell Culture, Genentech, 1 DNA Way, South San Francisco, California 94080; telephone: 1-650-467-3284; fax: 1-650-225-2006; e-mail: inn@gene.com

[2]Protein Analytical Chemistry, Genentech, 1 DNA Way, South San Francisco, California 94080

[3]Analytical Operations, Genentech, 1 DNA Way, South San Francisco, California 94080

ABSTRACT: To understand the diversity in the cell culture harvest (i.e., feedstock) provided for downstream processing, we compared host cell protein (HCP) profiles using three Chinese Hamster Ovary (CHO) cell lines in null runs which did not generate any recombinant product. Despite differences in CHO lineage, upstream process, and culture performance, the cell lines yielded similar cell-specific productivities for immunogenic HCPs. To compare the dynamics of HCP production, we searched for correlations between the time-course profiles of HCP (as measured by multi-analyte ELISA) and those of two intracellular HCP species, phospholipase B-like 2 (PLBL2) and lactate dehydrogenase (LDH). Across the cell lines, proteins in the day 14 supernatants analyzed by two-dimensional polyacrylamide gel electrophoresis (2D-PAGE) showed different spot patterns. However, subsequent analysis by liquid chromatography coupled with tandem mass spectrometry (LC-MS/MS) indicated otherwise: the total number of peptides and proteins identified were comparable, and 80% of the top 1,000 proteins identified were common to all three lines. Finally, to assess the impact of culture viability on extracellular HCP profiles, we analyzed supernatants from a cell line whose viability dropped after day 10. The amounts of HCP and PLBL2 (quantified by their respective ELISAs) as well as the numbers and major populations of HCPs (identified by LC-MS/MS) were similar across days 10, 14, and 17, during which viabilities declined from ~80% to <20% and extracellular LDH levels increased several-fold. Our findings indicate that the CHO-derived HCPs in the feedstock for downstream processing may not be as diverse across cell lines and upstream processes, or change as dramatically upon viability decline as originally expected. In addition, our findings show that high density CHO cultures (>10^7 cells/mL)—operated in fed-batch mode and exhibiting high viabilities (>70%) throughout the culture duration—can accumulate a considerable amount of immunogenic HCP (~1–2 g/L) in the extracellular environment at the time of harvest (day 14). This work also demonstrates the potential of using LC-MS/MS to overcome the limitations associated with ELISA and 2D-PAGE for HCP analysis.

Biotechnol. Bioeng. 2015;9999: 1–16.

KEYWORDS: CHO host cell protein; PLBL2; ELISA; LC-MS/MS; proteomics; orthogonal methods

Introduction

A key challenge in downstream processing of recombinant biopharmaceuticals is the removal of host cell proteins (HCPs). When present in the administered product even at low levels, HCPs may induce an undesired immune response (Singh, 2011). While many researchers have investigated various aspects of downstream processing that impact clearance of HCPs produced by Chinese Hamster Ovary (CHO) cells (e.g., Levy et al., 2014; McDonald et al., 2009; Shukla et al., 2008), few have taken their investigations to the upstream process (Grzeskowiak et al., 2009; Jin et al., 2010; Tait et al., 2011; Valente et al., 2015).

Three recent studies covering the upstream perspective highlighted the impact of culture viability on HCP profiles: (1) Tait et al. (2012) compared HCPs in supernatants generated by a null cell line (i.e., a cell line without the product coding gene), and by a recombinant IgG4-producing cell line. They reported significant increases in HCPs—immunogenic HCP levels as measured by enzyme-linked immunosorbent assay (ELISA), protein spot changes by two-dimensional polyacrylamide gel electrophoresis (2D-PAGE), and peak intensities by mass spectrometry (MS)—which they associated with viability decline upon increasing run duration. (2) Jin et al. (2010) studied the effects of multiple upstream process parameters on supernatants from a recombinant CHO cell line producing an Fc-fusion protein. They concluded that culture viability, also associated with increasing run duration, exerted the greatest impact on HCP patterns by two-dimensional fluorescence difference gel electrophoresis (2-D DIGE). (3) Grzeskowiak et al. (2009) contrasted the effects of clones (generated

Conflict of interest: The authors have no conflict of interest to declare.

Correspondence to: I. H. Yuk

Received 20 December 2014; Revision received 3 March 2015; Accepted 9 April 2015
Accepted manuscript online xx Month 2015;
Article first published online in Wiley Online Library (wileyonlinelibrary.com).
DOI 10.1002/bit.25615

simultaneously from a CHO DG44 host in the same transfection and cell line development process) with culture viability on HCPs in supernatants and found lower HCP levels in higher viability cultures. Using 2-D DIGE, they observed that the HCP patterns differed more between high and low viability cultures than between two clones expressing the same recombinant IgG product. However, these three recent studies did not investigate the impact on HCP profiles from using null cell lines that differ in their CHO parental origins. More recently, Lewis et al. (2013) reported genetic heterogeneity across six CHO cell lines derived from the CHO-K1, CHO DG44, and CHO-S lineages. Although these researchers had previously completed a comprehensive proteomic analysis of the CHO-K1 cell line (Baycin-Hizal et al., 2012), they did not further explore whether the differences in CHO genome across the six cell lines (Lewis et al., 2013) translated into appreciable differences in the proteome.

In our previous work (Krawitz et al., 2006), we studied HCPs from three null CHO cell lines sharing a close lineage: they were derived from the dihydrofolate reductase (DHFR)-deficient DUKX cell line isolated by Urlaub and Chasin (1980). The aim of our earlier study was to understand differences in cellular protein expression, but not in cell culture harvests. As such, HCP patterns by 2D-PAGE were comparable across the cell lines. The samples we tested then originated from cell pellets, and were not intended to represent the typical material harvested at the end of cell culture by removing the cells (i.e., feedstock), which would be supplied to downstream processing for purification.

In the present work, our first goal was to assess the diversity in HCPs—in terms of the number and composition of detectable HCP species as well as the total amount of immunogenic HCPs—in the feedstock for downstream processing using a variety of in-house cell lines cultured in their standard processes (Table I). Our second goal was to investigate the previously observed impact of culture viability on HCP profiles in supernatants (Grzeskowiak et al., 2009; Jin et al., 2010; Tait et al., 2011). Our third goal was to compare the findings from different orthogonal methods for HCP analysis (Tscheliessnig et al., 2013; Wang et al., 2009; Zhu-Shimoni et al., 2014). To this last end, we compared two traditional methods for characterizing HCPs—the quantitative, immunospecific approach of HCP ELISA and the qualitative, non-specific approach of 2D-PAGE—with the orthogonal method of liquid chromatography coupled with tandem MS (LC-MS/MS) that can identify specific HCPs present even at low levels (Reisinger et al., 2014).

To accomplish these goals, we focused our HCP characterization efforts primarily on the culture supernatant, which should include HCPs that were secreted during cell culture as well as those released into the culture fluid by cell lysis. To evaluate the range of potential HCP diversity in the cell culture harvests, while eliminating the confounding factor of recombinant gene expression, we selected three strains of null cells representing a broader CHO lineage than what we previously studied (Krawitz et al., 2006): a DUKX-derived cell line (Host 1), plus two CHO-K1 cell lines (Hosts 2 and 3) that underwent different media adaptations. Unlike our previous study (Krawitz et al., 2006), the upstream process (i.e., media and culture conditions) was not identical for the three cell lines. Specifically, the upstream process for each null cell line was based on the standard bioreactor process developed for recombinant cell lines derived from the same CHO host strain (Table I). This study did not decouple the effect of cell line from the effect of upstream process because our intent was to capture the maximum, not minimum, extent of HCP diversity that may be encountered at the start of downstream processing. However, for ease of discussion, we referred primarily to differences in cell line (i.e., Hosts 1–3) without emphasizing the corresponding differences in upstream process (Table I).

Materials and Methods

Cell Lines

The three null cell lines tested here originated from a common CHO ancestor: the CHO-K1 subclone (Kao and Puck, 1968) derived from CHO cells isolated by Puck et al. (1958). These null cell lines—which did not encode for any recombinant product genes—were referred to herein as Host 1, Host 2, and Host 3 because they represented three different CHO-K1 host strains. Host 1 was derived from a strain of dihydrofolate reductase-deficient DUKX cells that was previously referred to as DP12 cells (Hu et al., 2013; Krawitz et al., 2006). The DUKX (also known as DXB11 or DUKX-B11) cells were generated by mutagenizing the CHO-K1 subclone to create a missense mutation in one allele and a deletion in the other allele of the dihydrofolate reductase gene (Urlaub and Chasin, 1980). DP12 cells were developed by transfecting the DUKX cells with a plasmid containing the coding sequence for preproinsulin and adapting them to suspension growth in proprietary, chemically defined media. Host 1 was generated from DP12 cells by transfection with a plasmid containing dihydrofolate reductase. Hosts 2 and 3 were both generated by directly adapting the CHO-K1 cell line—obtained from the American Type Culture Collection (ATCC Cat. No. CCL-61)—to suspension growth in different series of proprietary, chemically defined media. In summary, each cell line was exposed to different culture conditions prior to cryopreservation. Frozen stocks of Hosts 1–3 were maintained in cell banks and subsequently

Table I. Differences in CHO cell lines and upstream processes used for null runs in 2 L bioreactors.

Cell line details	Host 1	Host 2	Host 3
CHO lineage	DUKX	CHO-K1	CHO-K1
Adaptation history[a]	Cell lines were adapted to grow in different media		
Production culture media[a]	Medium A	Medium B	Medium C
Nutrient feed[a] (on day 3)	Feed A	Feed A	Feed B[b]
Production process temperature shift (on day 3)	35°C	33°C	35°C

[a]All culture media used were chemically defined.
[b]An additional nutrient feed was supplied on day 7.

thawed and scaled up in shake flasks in preparation for HCP production studies.

Shake Flask Culture

A shake flask production culture was inoculated in a 250 mL Erlenmeyer flask (Corning) with 80 mL of Host 3 cells resuspended in 100% fresh chemically defined medium C at a viable cell density (VCD) of $\sim 1.2 \times 10^6$ cells/mL. The culture was agitated on an orbital shaker (150 rpm, 25 mm throw) in a humidified incubator maintained at 37°C with a 7% CO_2 overlay. On day 3, the culture was supplemented with a concentrated nutrient feed B at 1:5 (v/v) and maintained thereafter at 35°C. On day 6, the culture was used to generate three types of samples: (1) cell pellet, (2) supernatant, and (3) whole cell culture fluid (WCCF). To generate the cell pellet and supernatant samples, 10 mL of WCCF (i.e., a well-mixed sample of the entire cell culture content) was centrifuged (830 *g*, 10 min) in a 15 mL polypropylene conical tube (Corning). The resulting centrate was poured into another container and this clarified liquid represented the supernatant sample. The remaining cell pellet was resuspended in phosphate-buffered saline (10 mL) and centrifuged (830 *g*, 10 min), and the centrate was decanted. The washed cell pellet was resuspended in 10 mL of phosphate-buffered saline. This cell suspension represented the cell pellet sample.

The three types of samples were each subjected to one of the following treatments: (1) the sample was not further treated by freeze-thaw or sonication (Fresh); (2) the sample was sonicated (Sonication); (3) the sample was frozen and then thawed (Freeze-Thaw); (4) the sample was frozen, thawed, and then sonicated (Freeze-Thaw + Sonication). To sonicate a sample, the contents were subjected to a single 3 s pulse at 100% amplitude delivered by the microtip probe of a Q700 ultrasonic processor (Qsonica, LLC). To freeze-thaw a sample, the contents were frozen in a −80°C Forma 8600 Series freezer (Thermo Scientific), and thawed at room temperature. After each of the samples had undergone one of the four treatments, all the samples were diluted in an assay diluent containing 0.05% (v/v) Polysorbate 20 and stored at 2–8°C (for <24 h) until the samples were analyzed for HCP or PLBL2 concentrations by their respective ELISAs.

Bioreactor Cultures

Ten HCP production cultures were inoculated at ∼0.25% packed cell volume (PCV) in sparged 2 L stirred-tank bioreactors (Applikon). All three cell lines were cultured in replicate bioreactors totaling four for Host 1, three for Host 2, and three for Host 3. Culture pH, dissolved oxygen, and agitation were maintained at 7.0, 30% of air saturation, and 350 rpm, respectively, throughout the run duration. The cultivation temperature was 37°C for the first three days for all cell lines, but was shifted thereafter to 35°C for Hosts 1 and 3, and to 33°C for Host 2. Process setpoints were controlled by TruBio (Finesse Solutions). Three days post-inoculation, a concentrated nutrient feed was added to each culture at a ratio of 1:5 (v/v). Seven days post-inoculation, an additional feed was also provided for Host 3 cultures. Glucose was supplemented to each culture as needed, to avoid depletion. The composition of chemically defined production media and nutrient feeds, in combination with the process conditions, were unique to each cell line (Table I). All bioreactor runs were harvested on day 14, except for two runs with Host 3 that were harvested on day 17 to further assess the impact of low culture viability on HCP profiles.

Cell Culture Analyses

Culture samples taken from the bioreactors were analyzed immediately for VCD and viability (V) using either the Vi-Cell XR (Beckman Coulter) or the BioProfile FLEX Analyzer (Nova Biomedical); both cell counting devices used Trypan blue dye exclusion to assess culture viability. Cultures were also analyzed for PCV by centrifugation (830 *g*, 10 min) in calibrated sedimentation tubes (Kimble Chase). Cell growth was therefore represented by both VCD and percent packed cell volume (%PCV), in which the PCV measurement was normalized as a percentage of the culture volume. At-line analysis of culture samples for pH, dissolved oxygen, carbon dioxide partial pressure (pCO_2), glucose, lactate, and NH_4^+ concentrations were conducted using either the BioProfile FLEX Analyzer or the Bioprofile 400 analyzer (Nova Biomedical). Additional WCCF and culture supernatant samples were taken on days 4, 7, 10, 12, and 14 of each production run. To generate each supernatant sample, a WCCF sample was clarified by centrifugation (830 *g*, 10 min). The WCCF and supernatant samples were stored immediately at −80°C and subsequently thawed at room temperature for various analyses as described below.

HCP Quantitation by ELISA

The total amount of immunogenic HCP in CHO cell culture samples was quantified by a proprietary enzyme-linked immunosorbent assay (ELISA), recently detailed by Vanderlaan et al. (2015). This HCP ELISA was developed in-house for multi-product use across CHO cultures at Genentech (Krawitz et al., 2006) and has been used for monitoring HCP removal during purification (McDonald et al., 2009; Zeid et al., 2009).

PLBL2 Quantitation by ELISA

PLBL2 in CHO cultures was quantified by a proprietary in-house ELISA (Vanderlaan et al., 2015). This PLBL2 ELISA used polyclonal antibodies that were raised against CHO-derived recombinant PLBL2 in rabbits. The antibodies produced by the rabbits were purified by an affinity column in which PLBL2 was coupled to Glycerol CPG (Millipore).

LDH Quantitation by Colorimetric Assay

The enzymatic activity of lactate dehydrogenase (LDH) in culture supernatant was determined using an LDH-based cytotoxicity detection kit (Roche Diagnostics GmbH). This colorimetric assay was based on two enzymatic steps. First, the reduction of NAD^+ to NADH and H^+ was coupled to the LDH-catalyzed oxidization of lactate to pyruvate. Next, the diaphorase catalyst used the NADH and H^+ generated to reduce a pale yellow tetrazolium salt to a red formazan product. The absorption of the resulting formazan dye was measured at 490 nm using an ELISA reader, and the activity of

LDH in the culture supernatant was normalized to the activity from an LDH standard (Roche Diagnostics GmbH).

HCP Analysis by 2D-PAGE

Day 14 supernatant samples from bioreactor cultures were concentrated and then solubilized (5 M urea, 2 M thiourea, 2% (w/v) CHAPS, 2% (w/v) ASB-14, 2% (w/v) Zwittergent 3–10, 1% (w/v) DTT, 2% (w/v) Bio-Lyte 8/10) to a final protein concentration of 7–10 mg/mL. 2D-PAGE was performed on the samples as described (Champion et al., 2001). In brief, 18 cm pH 3–10 linear immobilized pH gradient strips (Bio-Rad) were rehydrated overnight; isoelectric focusing was conducted for a total of 69 kV h to achieve first-dimensional separation; sodium dodecyl sulfate polyacrylamide gel electrophoresis was conducted using the ISO-DALT system (GE Healthcare) for second-dimensional separation (~10–160 kDa) on precast 9–18% gradient gels measuring 20 cm × 25 cm × 1.5 mm (Jule, Inc.). Each supernatant sample (~120 μg protein) was run in triplicate gels. After electrophoresis, the gels were fixed and the proteins were stained with SYPRO Ruby (Life Technologies) as detailed by Nishihara and Champion (2002). The resulting gel images were acquired by ChemiDoc MP (Bio-Rad Laboratories) and Delta2D v4.5.1 software (DECODON GmbH) was used to create a single composite image for each sample.

To compare the gel images between day 14 supernatant samples originating from different cell lines (i.e., Hosts 1–3), six replicate gels from each cell line were used to create a single representative 2D-PAGE profile of HCPs for that cell line. Each spot on the resulting composite gel (created using the "union fusion" algorithm on Delta2D) represented the mean normalized volume for that spot across replicate gels. The images were not manually edited, and neither spot filtering nor spot matching was applied in creating the composite gel images. The resulting digital composite gel for a cell line was then overlaid with the corresponding digital composite gel for another cell line. Different cell lines were depicted in different colors in these overlaid composite gel images to facilitate pairwise comparisons of HCP expression profiles.

HCP Analysis by LC-MS/MS

Supernatant samples generated by replicate 2 L bioreactors (i.e., biological replicates) were analyzed for each cell line, and each sample was analyzed in duplicate LC-MS/MS runs. In preparation for LC-MS/MS analysis, supernatant samples were concentrated to ~5 mg/mL using centrifugal filter units (Amicon) with a 10 kDa molecular weight cutoff. Approximately 500 μg of the protein retentate was digested with trypsin as previously described (Yu et al., 2011). The digested protein mixture (40 μg) was separated by reversed-phase ultra-performance liquid chromatography on an ACQUITY UPLC H-Class system (Waters Corporation) with a 2.1 × 150 mm ACQUITY UPLC CSH column (130 Å, 1.7 μm). The separation was performed at 60°C with a flow rate of 0.3 mL/min, starting with a 100% aqueous mobile phase (0.1% formic acid), ramping to 40% acetonitrile (0.1% formic acid) over 45 min, and followed by a 5 min wash in 95% acetonitrile before re-equilibration in initial aqueous conditions. Online MS analysis was performed using a TripleTOF 5,600 + mass spectrometer (AB SCIEX) collecting MS and tandem MS (MS/MS) data in Information Dependent Acquisition mode with the top 20 most abundant precursor ions chosen for MS/MS peptide fragmentation. Dynamic exclusion was set to 10 s and +1 charged ions were excluded from the MS/MS analysis. The mass accuracy was 5 ppm and the precursor ion mass tolerance for the subsequent database search was 0.05 Da.

LC-MS/MS data files were analyzed using the ProteinPilot protein identification software version 4.5 (AB SCIEX) to search against the UniProt database (www.uniprot.org; Proteome ID UP000001075) for canonical and isoform sequence data on Cricetulus griseus (Chinese hamster). Two technical replicates were combined from each culture sample for database searches. Proteins were considered positively identified if two or more unique peptide sequences were found at the >95% confidence level and the proteins satisfied the false discovery rate criterion of 1%. The proteins identified were compared using the ProteoIQ comparative proteomic analysis software version 2.7 (PREMIER Biosoft).

Total spectral counts for each sample were normalized by comparison to total spectral counts obtained in all biological replicates. The normalized spectral count for each protein was used as a semi-quantitative measure to rank proteins by abundance, with higher spectral counts indicating greater protein abundance. Analysis of HCP composition between samples was performed by comparing the list of proteins identified in each sample, ranked from highest to lowest by normalized spectral counts. The top 1,000 ranked proteins in each sample were compared to assess the amount of overlap between the HCP populations when increasing the depth of coverage of the CHO proteome.

Calculations

The cell-specific productivity with respect to HCP (Q_{HCP}) for each cell line was estimated from the relationship between HCP concentration ([HCP]), culture viability (V) and volumetric packed cell volume (vol.PCV):

$$[HCP](t) = Q_{HCP} \int_0^t V \bullet vol.PCV dt \quad (1)$$

[HCP] was measured in both the culture supernatant and the WCCF using the HCP ELISA, and vol.PCV was measured in units of L of packed cells per L of culture. The time integral in equation (1) was approximated as the volumetric integrated viable packed cell volume (vol.IVPCV) using the multiple-application trapezoidal rule (Chapra and Canale, 1988):

$$\int_0^t V \bullet vol.PCV dt \approx vol.IVPCV(t) \quad (2)$$

From the plot of [HCP](t) versus vol.IVPCV(t), Q_{HCP} was estimated in units of g of HCP per mL of viable packed cells per day (g mL-viable cell^{-1} day^{-1}) from the slope of the linear regression.

In an analogous manner, cell-specific productivity with respect to PLBL2 (Q_{PLBL2}) for each cell line was assessed by applying equation (2) to the following relationship:

$$[PLBL2](t) = Q_{PLBL2} \int_0^t V \bullet vol.PCV dt \qquad (3)$$

Q_{PLBL2} was estimated in units of g of PLBL2 per mL of viable packed cells per day (g mL-viable cell^{-1} day^{-1}) using the slope of the linear regression generated from plotting [PLBL2](t) versus vol.IVPCV(t).

To minimize complications with estimating cell-specific productivity in low viability cultures, only data obtained from cultures with viabilities >70% were used to calculate Q_{HCP} and Q_{PLBL2}.

Statistical Analysis

Statistical analyses were performed using JMP 11.0 software (SAS Institute Inc.). For each linear regression generated, the linear fit was assessed for statistical significance ($P < 0.01$) and correlation of determination (R^2) by one-way analysis of variance (ANOVA). The slopes of the regression lines for Hosts 1–3 cultures were further assessed for differences by analysis of covariance, unequal slopes (ANCOVA). Data for Hosts 1–3 were fitted to a linear model of the form $y = a + bx + c(x^*host)$. If the interaction term, x*host, showed $P < 0.01$, the slopes were considered to be significantly different across Hosts 1–3. ANOVA was also used to compare data across cell lines (i.e., Hosts 1–3) as well as data across culture duration within a cell line (i.e., days 10, 14, and 17 for Host 3) to search for significant differences ($P < 0.01$).

Results and Discussion

Relationship Between Supernatant and WCCF

To investigate the relationship between supernatant and WCCF samples, as well as the impact of different treatment methods on the immunogenic HCP and PLBL2 content of samples, we tested Host 3 cells from a shake flask production culture. The viability and VCD for the day 6 culture used to generate the different sample types were 97% and 1.1×10^7 cells/mL, respectively. Prior to the addition of assay diluent for analyses by HCP and PLBL2 ELISAs, the sonicated samples derived from cell pellets and WCCF were inspected under a microscope to verify complete cell lysis.

Within a given type of culture sample (i.e., cell pellet, supernatant, or WCCF), the immunogenic HCP (Fig. 1A) or PLBL2 (Fig. 1B) concentrations were comparable, irrespective of the sample treatment method. These findings indicate that the addition of assay diluent containing 0.05% (v/v) Polysorbate 20 to the samples prior to HCP and PLBL2 analyses by ELISA was as effective as sonication in releasing HCPs and PLBL2 from cell pellets and WCCF. They also indicate that the freeze-thaw method did not impact HCP and PLBL2 measurements relative to the other sample treatment methods. Additional testing of these different sample treatment methods using several recombinant CHO cell lines (derived from the same CHO origins as Hosts 1–3) further

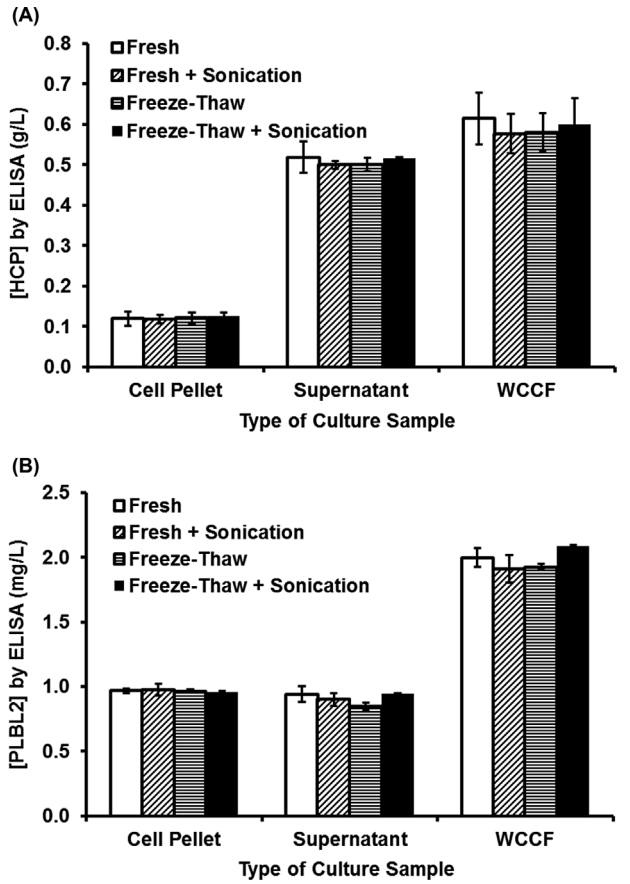

Figure 1. Comparison of sample treatment methods on (**A**) HCP, and (**B**) PLBL2 measured in cell pellet, supernatant, and WCCF samples. Four types of treatment methods were evaluated using samples taken from a Host 3 culture: (1) no freezing or sonication (Fresh); (2) sonication only (Sonication); (3) freezing to −80°C followed by thawing at room temperature (Freeze-Thaw); and (4) freezing to −80°C followed by thawing at room temperature and sonication (Freeze-Thaw + Sonication). Error bars represent one standard deviation from the mean for three technical replicates.

corroborated these conclusions (data not shown). Therefore, for ease and consistency of operation, subsequent studies used samples that were treated with the freeze-thaw method.

WCCF samples, comprised of cells and supernatant, were intended to represent the well-mixed contents of the culture vessel. Supernatant samples should be cell-free, and contain HCPs released into the extracellular environment from secretion or cell lysis, or both. Based on the principle of mass balance, the HCP concentration in the WCCF sample should approximate the sum of the HCP concentrations in the cell pellet and the supernatant samples. This mass balance principle should also apply for PLBL2. The immunogenic HCP and PLBL2 concentrations measured in the cell pellet, supernatant, and WCCF samples were consistent with this assumption (Fig. 1). Additional testing using several recombinant CHO cell lines (covering the same range of CHO strains as Hosts 1–3) also supported this mass balance principle for the distribution of immunogenic HCP and PLBL2 across the cell pellet, supernatant, and WCCF samples (data not shown). Therefore, to avoid the extra sample manipulations required to

generate cell pellet samples, subsequent studies used WCCF samples to estimate the combined cellular and extracellular content of immunogenic HCPs and PLBL2.

Cell Culture Profiles

Hosts 1–3 showed distinct growth (as measured by VCD and PCV) and viability profiles (Fig. 2) when cultured in their respective standard bioreactor processes (Table I). Within a cell line, the differences between the VCD and PCV profiles illustrate the contribution of viability to VCD. Across the cell lines, the relative differences in growth profiles illustrate the contribution of cell size to PCV. For example, Host 1 cells were, on average, smaller than Host 2 cells. To minimize the effects of different cell sizes, subsequent cell-specific productivity calculations considered only PCV (in conjunction with culture viability) instead of VCD.

The three null cell lines also displayed distinct extracellular lactate, NH_4^+, osmolality, and pCO_2 profiles (Fig. 3). The decline in viability for Host 3 cultures, especially evident after day 10, was associated with continuous lactate production (Fig. 3A), which would elevate culture osmolality (Fig. 3C) because of the base addition required to maintain culture pH. Such high levels of extracellular lactate ($\geq$10 g/L) and osmolality (>500 mOsm/kg) should be detrimental to viability and growth for mammalian cells (Omasa et al., 1992; Zhu et al., 2005). To assess the effects of prolonged cultivation at low viability on HCP profiles, the run duration was extended from day 14 to day 17 for two Host 3 cultures.

HCP Profiles by ELISA

The time-course profiles for HCP (measured by ELISA) in both the supernatant (Fig. 4A) and WCCF (Fig. 4B) from the null production runs were unique to each cell line: HCP levels increased with culture duration for Host 1 and Host 2 cultures, but did not show a clear increase after day 10 for Host 3 cultures, when viability profiles diverged (Fig. 2C).

The HCP time-course profiles for Host 3 cultures differed from the findings by Tait et al. (2012) in two aspects. First, Tait et al. found that when viabilities for a null CHO cell line (identified as Null8) decreased from ~70% (day 12) to 35% (day 14), HCP levels increased from 119 ± 11 mg/L to 148 ± 5 mg/L, in contrast to the observed plateau in HCP levels we observed for Host 3 cultures after day 10 (Fig. 4A). Second, Tait et al. reported HCP levels (using a commercial ELISA kit) from Null8 cultures that were an order of magnitude lower than those detected in Host 3 cultures using our proprietary ELISA, even though Null8 cultures achieved comparable peak VCDs (>8 × 10^6 cells/mL between days 7 and 10) to our Host 3 cultures (Fig. 2A). By contrast, the HCP levels produced by our null runs (~1–2 g/L) fell well within an order of magnitude of one another (across Hosts 1–3) in spite of differences in upstream process (Table I) and culture performance (Figs. 2 and 3). The HCP levels in our null runs also fell within the product titer range for the IgG1s produced (~1–3 g/L) by some of our recombinant CHO cell lines derived from the same host strains and cultured using similar processes (Hsu et al., 2012; Yuk et al., 2015).

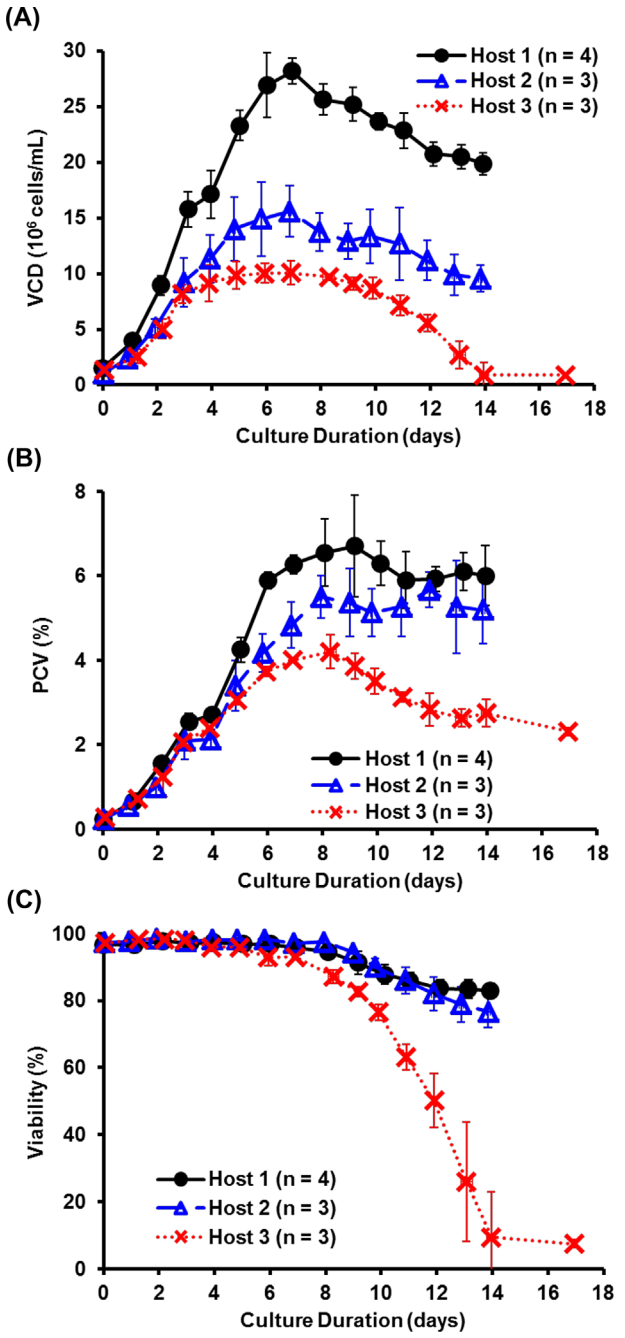

Figure 2. Comparison of (**A**) VCD, (**B**) PCV, and (**C**) culture viability profiles for null runs with three CHO cell lines (Hosts 1–3). Two of the three replicate runs for Host 3 were extended to day 17. Error bars represent one standard deviation from the mean for replicate runs using the same cell line in 2 L bioreactors.

To differentiate the contributions from cell growth and viability from that of Q_{HCP} towards the HCP time-course profiles, we plotted HCP concentration in the supernatant (Fig. 4C) and in the WCCF (Fig. 4D) as a function of vol.IVPCV for each cell line. The resulting Q_{HCP} values—obtained from the slope of the linear regression—were comparable across Hosts 1–3: the *P*-values by ANCOVA for the three slopes were 0.87 (Fig. 4C) and 0.32 (Fig. 4D) based on

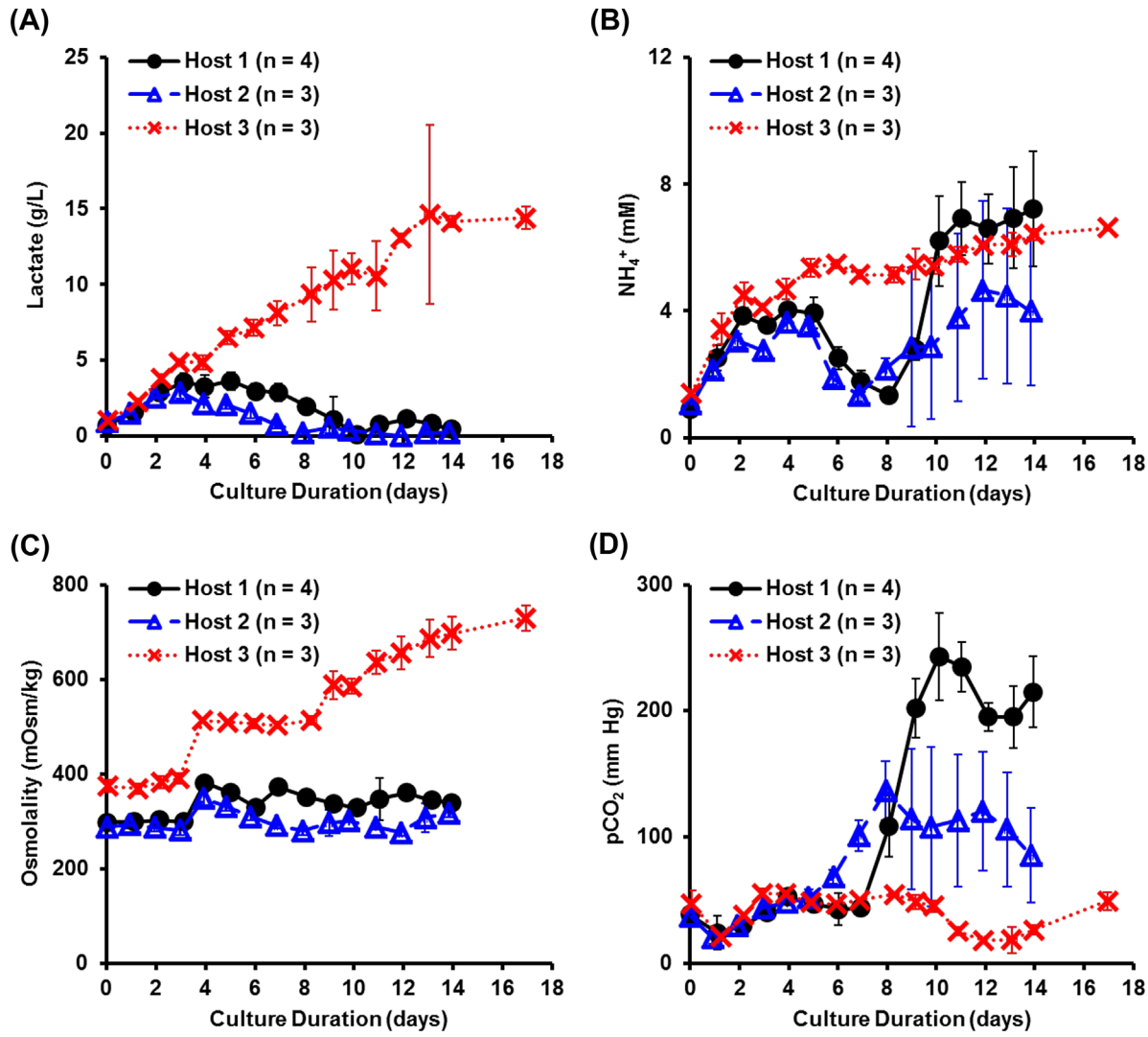

Figure 3. Comparison of extracellular (**A**) lactate, (**B**) NH_4^+, (**C**) osmolality, and (**D**) pCO_2 profiles for null runs with three CHO cell lines (Hosts 1–3). Two of the three replicate runs for Host 3 were extended to day 17. Error bars represent one standard deviation from the mean for replicate runs using the same cell line in 2 L bioreactors.

measurements for supernatant and WCCF samples, respectively. Therefore, the differences in HCP concentrations by ELISA across these three null cell lines resulted from differences in cell growth and viability instead of differences in Q_{HCP}. In theory, the Q_{HCP} value obtained for a specific CHO cell line can be used in combination with cell growth and viability profiles to estimate the final immunogenic HCP levels at the time of harvest for future production runs using the same cell line and upstream process. However, such an estimate would not account for potential Q_{HCP} changes with cell age for that cell line (Valente et al., 2015).

PLBL2 Profiles by ELISA

The HCP profiles by ELISA across Hosts 1–3 focus on a wide population of HCPs and do not illustrate how the abundance of an individual HCP species may change with culture duration. Given our interest in PLBL2—an HCP species present in CHO cultures that can interact with certain recombinant humanized monoclonal antibodies (Vanderlaan et al., 2015)—we chose PLBL2 as our HCP of interest to profile in these null runs. The PLBL2 time-course profiles (measured by PLBL2-specific ELISA) in both the supernatant (Fig. 5A) and WCCF (Fig. 5B) were distinct across Hosts 1–3.

As revealed by PLBL2 levels in the culture supernatant (Fig. 5C), cell-specific PLBL2 productivity (Q_{PLBL2})—estimated by the slope of the linear regression of PLBL2 versus vol.IVPCV—did not vary significantly across Hosts 1-3 ($P = 0.38$ by ANCOVA). The considerable spread in the data used for generating the linear regressions, especially for Host 3 (Fig. 5C), lowered the reliability of the Q_{PLBL2} values estimated for each cell line. Since PLBL2 is a lysosomal protein (Jensen et al., 2007; Lakomek et al., 2009), we expect it to be retained inside viable cells. Taking the cellular content of PLBL2 into consideration, Q_{PLBL2} based on PLBL2 levels in the WCCF (Fig. 5D) differed significantly across Hosts 1–3 ($P < 0.01$ by ANCOVA); average cell-specific production of PLBL2

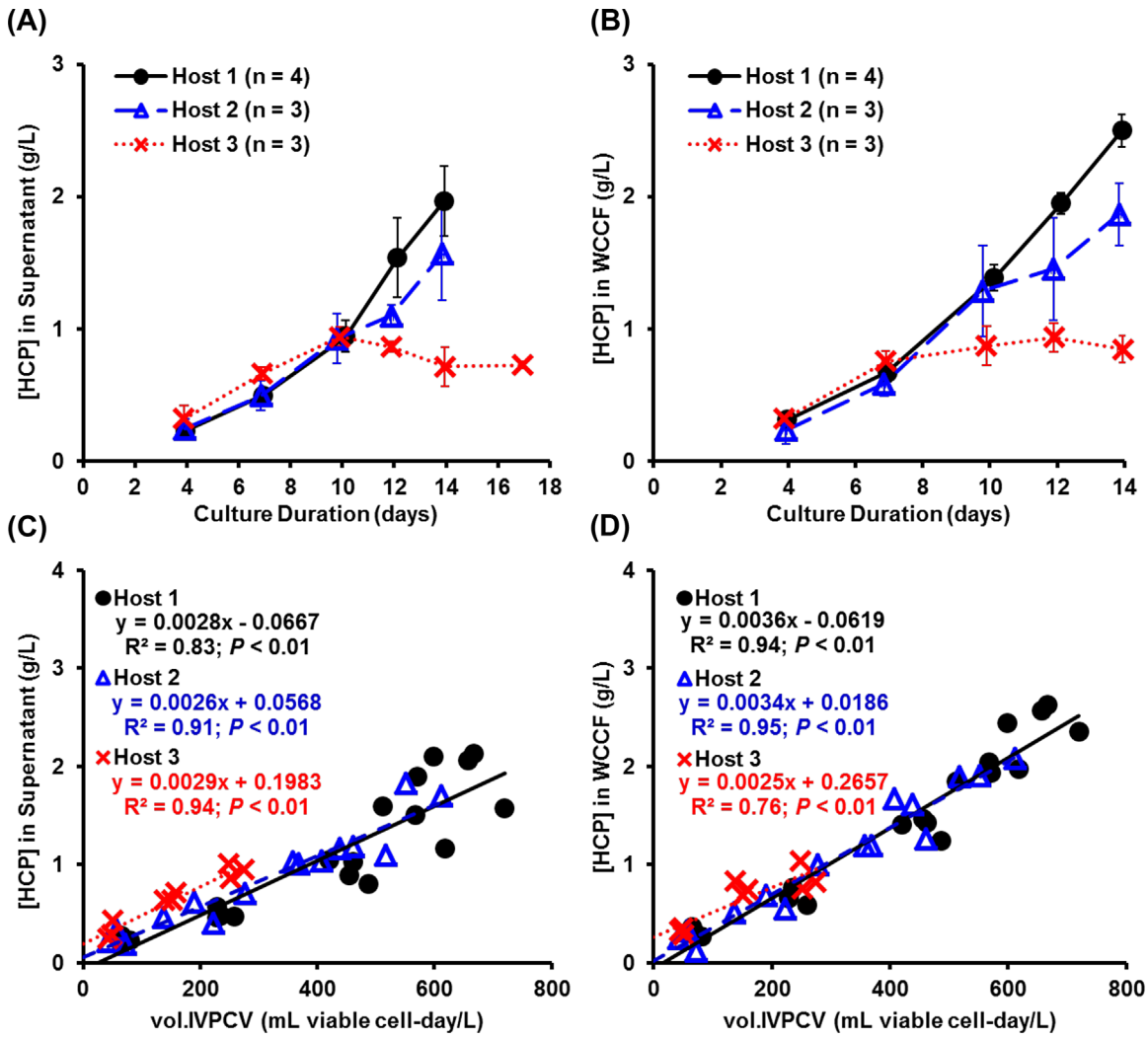

Figure 4. Comparison of HCP concentration in null runs with three CHO cell lines (Hosts 1–3), each cultured in replicate 2 L bioreactors. HCP concentration was plotted as a function of culture duration in (**A**) culture supernatant, and (**B**) WCCF. HCP concentration was plotted as a function of cumulative viable packed cell volume, represented by vol. IVPCV, in (**C**) culture supernatant, and (**D**) WCCF. HCP concentration was determined by HCP ELISA. Error bars represent one standard deviation from the mean for replicate runs using the same cell line. Slopes generated by the linear regression in the plots of HCP versus vol.IVPCV represent the cell-specific HCP productivity (Q_{HCP}).

in Host 1 cultures was almost fivefold higher than in Host 3 cultures. Similar to the concept described for Q_{HCP}, if we assume that each cell line has its own characteristic Q_{PLBL2} value, then this value can be used with the IVPCV value to estimate the PLBL2 levels in a production run using the same cell line and upstream process. In addition to demonstrating the inherent ability of our CHO-K1 cell lines to produce PLBL2, our findings also demonstrate that the extracellular presence of PLBL2 does not depend on the secretion of recombinant product.

Correlations between HCP, PLBL2, and LDH

PLBL2 is known to be reactive in the CHO-based HCP ELISA used for this study (Vanderlaan et al., 2015). To compare the contribution of PLBL2 towards the total level of immunogenic HCP across Hosts 1–3 cultures, PLBL2 concentration (obtained by the PLBL2 analyte-specific ELISA) was plotted against HCP concentration (obtained by the multi-analyte HCP ELISA) in the culture supernatant (Fig. 6A) and WCCF (Fig. 6B). The resulting slope of the linear regression for each cell line provided the estimate for the average mg of PLBL2 present per g of HCP. The differences in slope across cell lines were statistically significant ($P < 0.01$ by ANCOVA) whether the analysis was performed on the supernatant or WCCF. However, the actual differences in slope were relatively small and therefore, these differences are not likely to be biologically significant. In Hosts 1–3 cultures, PLBL2 contributed to <1% of the total HCP measured by ELISA. For a multi-analyte ELISA used to monitor a wide array of HCPs, this level of reactivity to a single analyte is expected.

At a given duration for each culture, the difference in HCP concentration between the WCCF and supernatant samples should correspond to the cellular HCP concentration. Therefore,

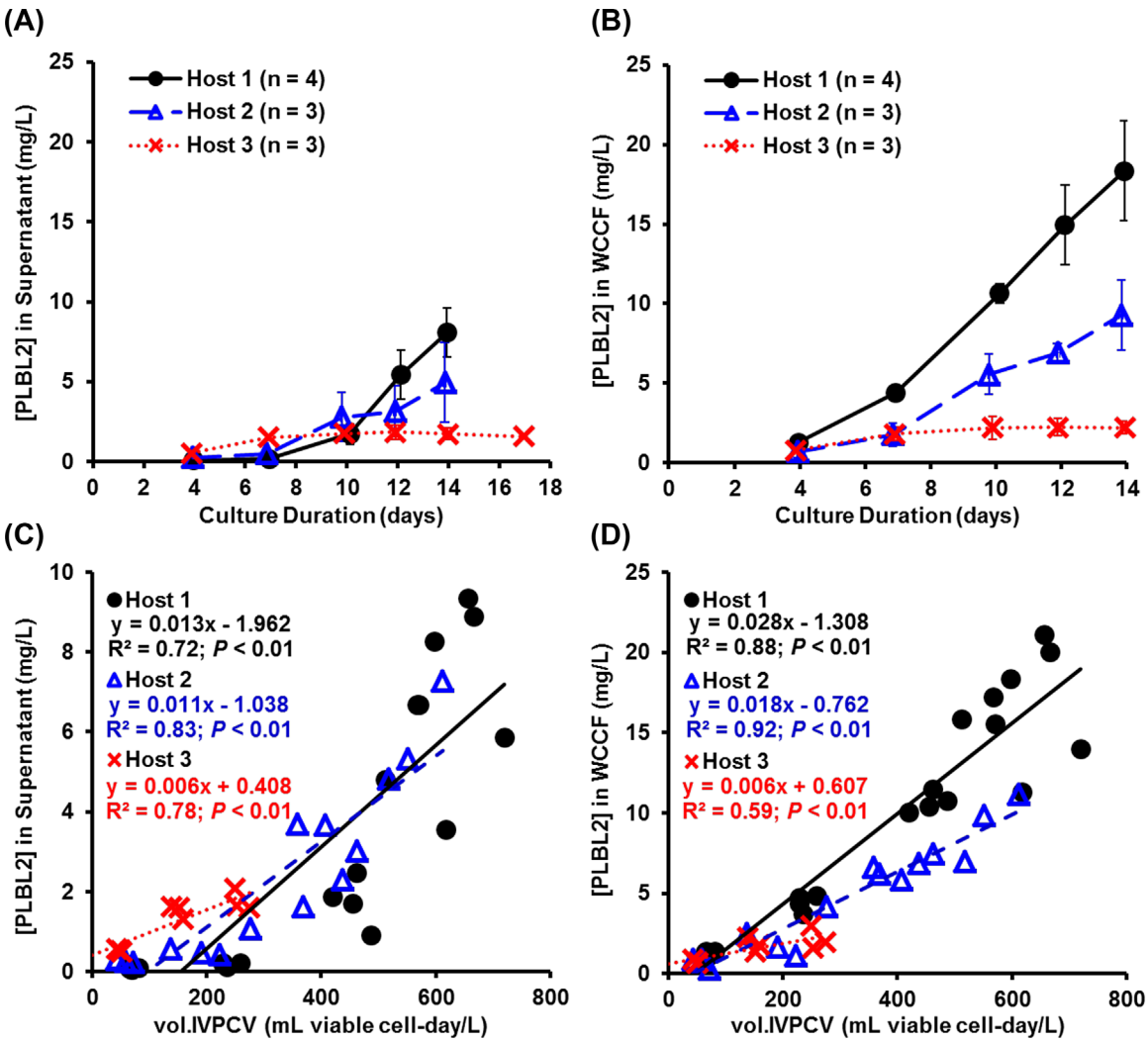

Figure 5. Comparison of PLBL2 concentration in null runs with three CHO cell lines (Hosts 1–3), each cultured in replicate 2 L bioreactors. PLBL2 concentration was plotted as a function of culture duration in (**A**) culture supernatant, and (**B**) WCCF. PLBL2 concentration was plotted as a function of cumulative viable packed cell volume, represented by vol.IVPCV, in (**C**) culture supernatant, and (**D**) WCCF. PLBL2 concentration was determined by PLBL2 ELISA. Error bars represent one standard deviation from the mean for replicate runs using the same cell line. Slopes generated by the linear regression in the plots of PLBL2 versus vol.IVPCV represent the cell-specific PLBL2 productivity (Q_{PLBL2}).

the slope of the linear regression from plotting HCP in the supernatant versus HCP in the WCCF should provide the average fraction of HCP present in the supernatant relative to the entire culture content (Fig. 6C). Averaged over the run duration, ~73–86% of the total amount of immunogenic HCPs in the cultures were located in the supernatants; these numbers did not differ significantly across the three cell lines ($P = 0.61$ by ANCOVA). By extending this analysis to PLBL2 (Fig. 6D), we infer that ~47–75% of the total PLBL2 in the cultures were located in the supernatants. For all bioreactor runs ($n = 10$), >60% of the total amount of HCPs and >30% of the total amount of PLBL2 in the cultures were located in the supernatant at day 14. We have not encountered reports of similar head-to-head comparisons of total HCP content or the concentration of a specific lysosomal protein in cell-free supernatant versus cell-containing WCCF samples. Despite the absence of literature reports on such comparisons, we had expected a smaller fraction of total HCP—and of PLBL2 in particular—to be located in the supernatant, especially in the highly viable cultures for Hosts 1 and 2.

We assumed PLBL2 was not actively secreted by viable cells because there are no known pathways for PLBL2 secretion. Based on this assumption, cell lysis would need to occur, even in the highly viable cultures for Hosts 1 and 2, to account for the unexpectedly large fraction of PLBL2 present in the supernatant relative to the WCCF at the time of day 14 harvest (Fig. 6D). To gauge the extent of cumulative cell lysis in the null runs, we analyzed the levels of lactate dehydrogenase (LDH) in the supernatant samples. LDH is an intracellular enzyme that should only be released upon loss of cell membrane integrity; supernatant LDH measurements can reveal low levels of cell

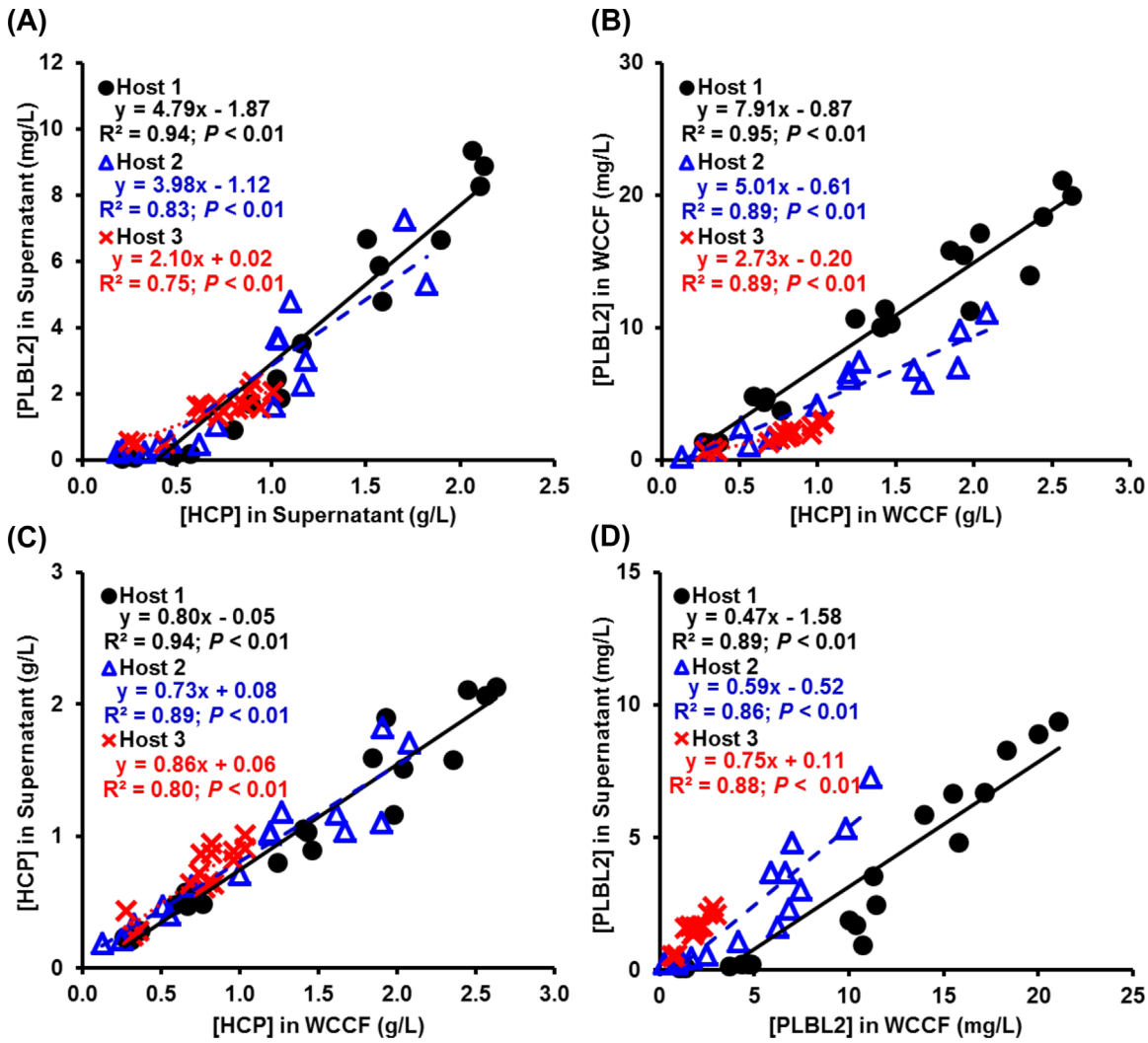

Figure 6. Correlations in HCP and PLBL2 concentrations for null runs with three CHO cell lines (Hosts 1–3). PLBL2 concentration as a function of HCP concentration for culture samples from (**A**) supernatant, and (**B**) WCCF. Concentration in supernatant as a function of concentration in WCCF for (**C**) HCP, and (**D**) PLBL2. The number of replicate 2 L bioreactors used to generate the data shown was four for Host 1, three for Host 2, and three for Host 3. HCP concentration was determined by HCP ELISA; PLBL2 concentration was determined by PLBL2 ELISA. Equations represent the linear regression generated using data for each cell line.

lysis that may not be detectable by Trypan blue dye exclusion (Petersen et al., 1988; Racher et al., 1990).

The LDH concentrations in the supernatants on day 14 (Fig. 7A) were comparable across Hosts 1–3 ($P = 0.20$ by ANOVA), despite the significantly lower final viabilities observed for Host 3 cultures. This apparent contradiction may be explained by the significantly higher cell growth in Host 1 and 2 relative to Host 3 cultures (Fig. 2): even if the fraction of cells that lysed in Host 1 and 2 cultures were smaller than in Host 3 cultures, the total number of lysed cells may be comparable across Host 1–3 cultures by the end of the production runs. These LDH observations highlight the possibility that the extent of cumulative cell lysis can be substantial in high cell density fed-batch CHO cultures, despite high viability readings by Trypan blue dye exclusion.

Over the course of culture, LDH concentration correlated negatively with viability (Fig. 7B), and positively with immunogenic HCP (Fig. 7C) and PLBL2 (Fig. 7D) levels; for each set of correlations, the linear regression slopes differed across Hosts 1–3 ($P < 0.01$ by ANCOVA). The increase in LDH with culture duration across Hosts 1–3 provides evidence that cell lysis was occurring, even in the Host 1 and 2 cultures with high viabilities (>70%). As a result of this cumulative cell lysis, we would expect a corresponding accumulation of intracellular proteins in the culture supernatant over run duration. However, our findings not rule out other currently unknown pathways for the release of PLBL2 from viable cells.

The WCCF analyses for Host 3 cultures corroborates the expectation that even if complete cell lysis occurred at day 14, the extracellular levels of HCP and PLBL2 would increase minimally because cell-associated HCPs (Fig. 4B) and PLBL2 (Fig. 5B) were outweighed by their counterparts in the supernatant. This applies not only for Host 3 cultures, but also Host 1 and 2 cultures at the typical time of harvest (day 14). Therefore, operational issues

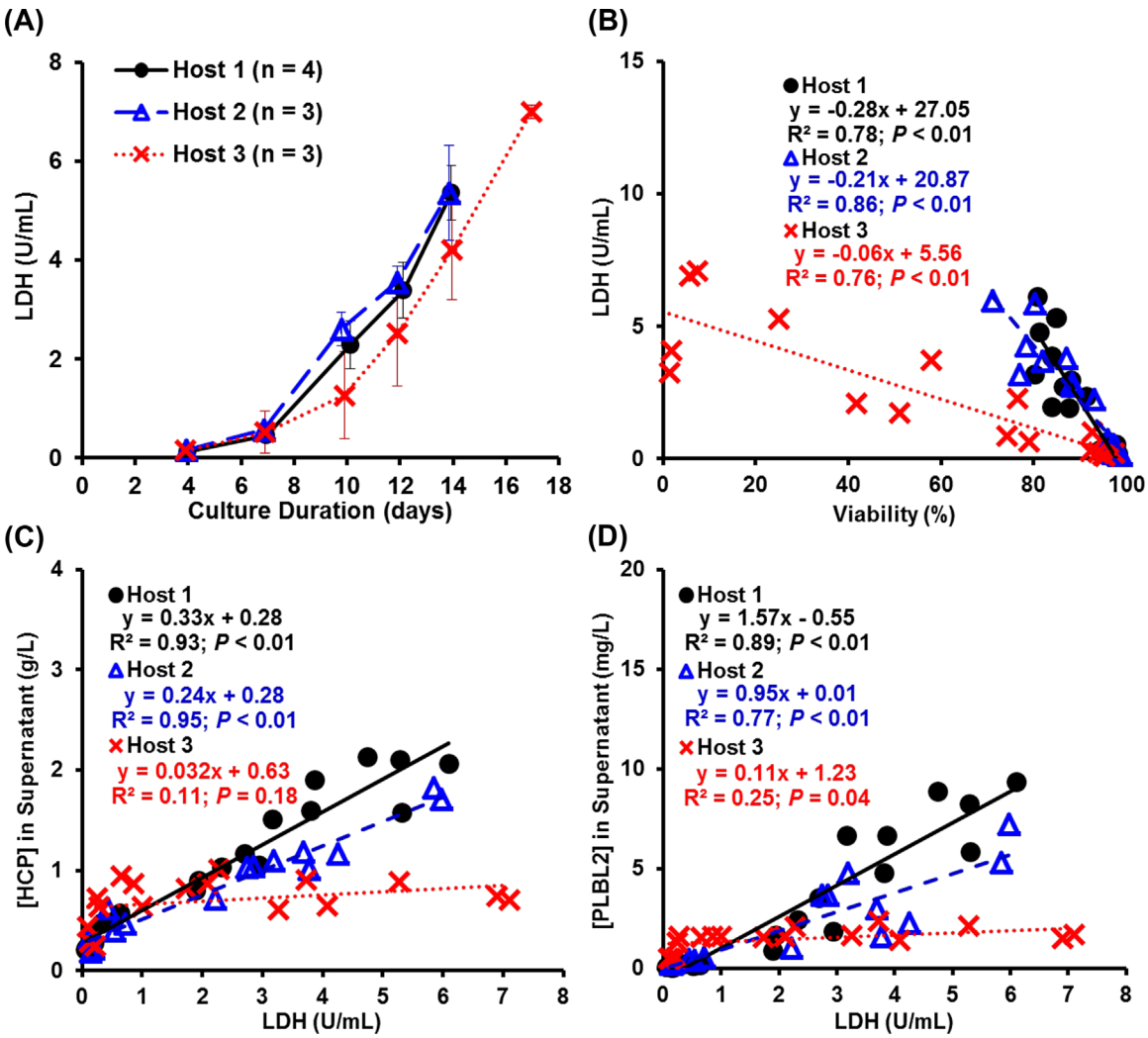

Figure 7. Comparison of extracellular LDH concentration in null runs with three CHO cell lines (Hosts 1–3), each cultured in replicate 2 L bioreactors. LDH concentration was plotted as a function of (**A**) culture duration, and (**B**) culture viability. Extracellular concentrations of (**C**) HCP, and (**D**) PLBL2 were plotted as a function of LDH concentration. Error bars represent one standard deviation from the mean for replicate runs using the same cell line in 2 L bioreactors. Equations represent the linear regression generated using data for each cell line.

during the harvest operation that lead to additional cell lysis for the range of CHO cultures tested here should only fractionally increase the total amount of immunogenic HCP in the feedstock for downstream processing.

The extracellular HCP (Fig. 4A) and PLBL2 (Fig. 5A) time-course profiles observed for these null cell lines resemble the extracellular IgG1 product titer profiles previously observed for our recombinant CHO cell lines (Hsu et al., 2012; Yuk et al., 2015): in cultures with consistently high (>70%) viabilities, IgG1 concentrations would continuously increase; in cultures that drop in viability, the start of the plateau in IgG1 concentrations would coincide with onset of a decline in viability. In those recombinant cell lines, extracellular LDH levels would continuously increase, regardless of the viability profiles (data not shown). Therefore, the apparent disparity in extracellular profiles for immunogenic HCPs (Fig. 4A) and PLBL2 (Fig. 5A) versus LDH (Fig. 6A) after day 10 in Host 3 cultures is consistent with our prior observations for extracellular profiles of IgG1 product titer and LDH in recombinant CHO cell lines with viability decline.

HCP Profiles by 2D-PAGE

Although ELISA is the most practical and widely used method for HCP analysis (Wang et al., 2009), and considered to be the gold standard (Tscheliessnig et al., 2013), there are limitations associated with multi-analyte immunoassays (Vanderlaan et al., 2015; Zhu-Shimoni et al., 2014). In light of these limitations, we further analyzed the HCPs generated by the three null cell lines via the well-established orthogonal method of 2D-PAGE (Champion et al., 2001; Chevalier 2010; Rabilloud et al., 2010).

Since our primary goal for this work was to understand potential differences in the starting load for downstream processing, we

chose to focus the labor-intensive 2D-PAGE analysis on the most relevant samples. We selected day 14 supernatant samples because they represent the typical culture duration and type of feedstock for downstream processing. To discern between variability within biological replicates and variability across Hosts 1–3, we compared 2D-PAGE images for day 14 culture supernatants from duplicate bioreactors for each cell line (Fig. 8). The 2D-PAGE patterns differed more noticeably between the cell lines than between biological

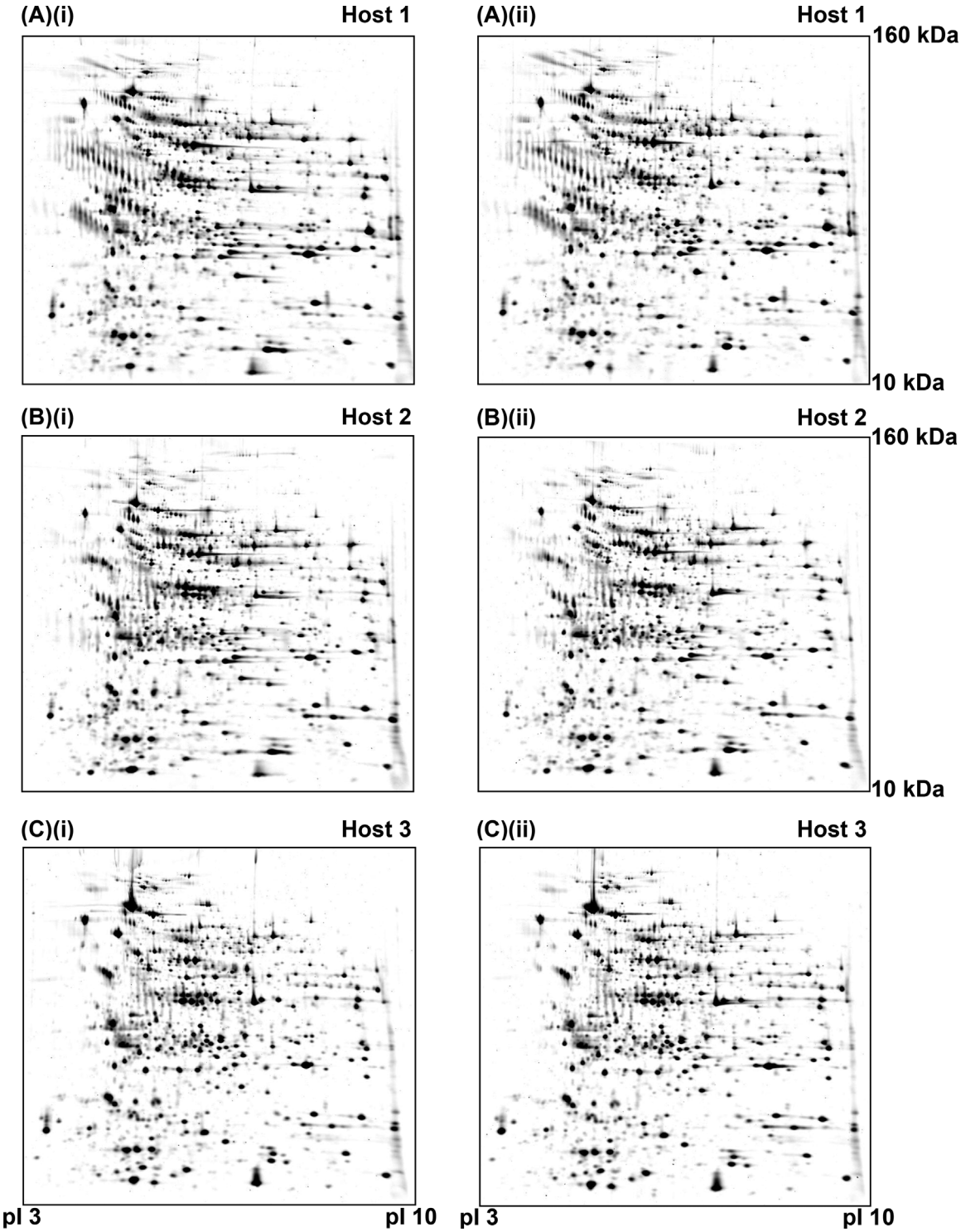

Figure 8. Comparison of 2D-PAGE images for HCPs from three CHO cell lines: (**A**) Host 1, (**B**) Host 2, and (**C**) Host 3. Day 14 culture supernatants from null runs in 2 L bioreactors were stained with SYPRO Ruby. Each image represents the composite of technical replicates (triplicate gels) from (**i**) one bioreactor, and (**ii**) a duplicate bioreactor.

replicates, as confirmed by pairwise comparison of the super-imposed 2D-PAGE images from different cell lines (Fig. 9). These differences are more pronounced when comparing Host 1 to either Host 2 (Fig. 9A) or Host 3 (Fig. 9C). Given that Hosts 2 and 3 share the closest lineage amongst the three null CHO cell lines (Table I), whereas Hosts 1 and 2 share the most similar culture media and cell culture performance (Figs. 2 and 3), cell line origin appears to have a greater impact on HCP patterns than upstream process (i.e., media and culture conditions) and culture performance (including viability).

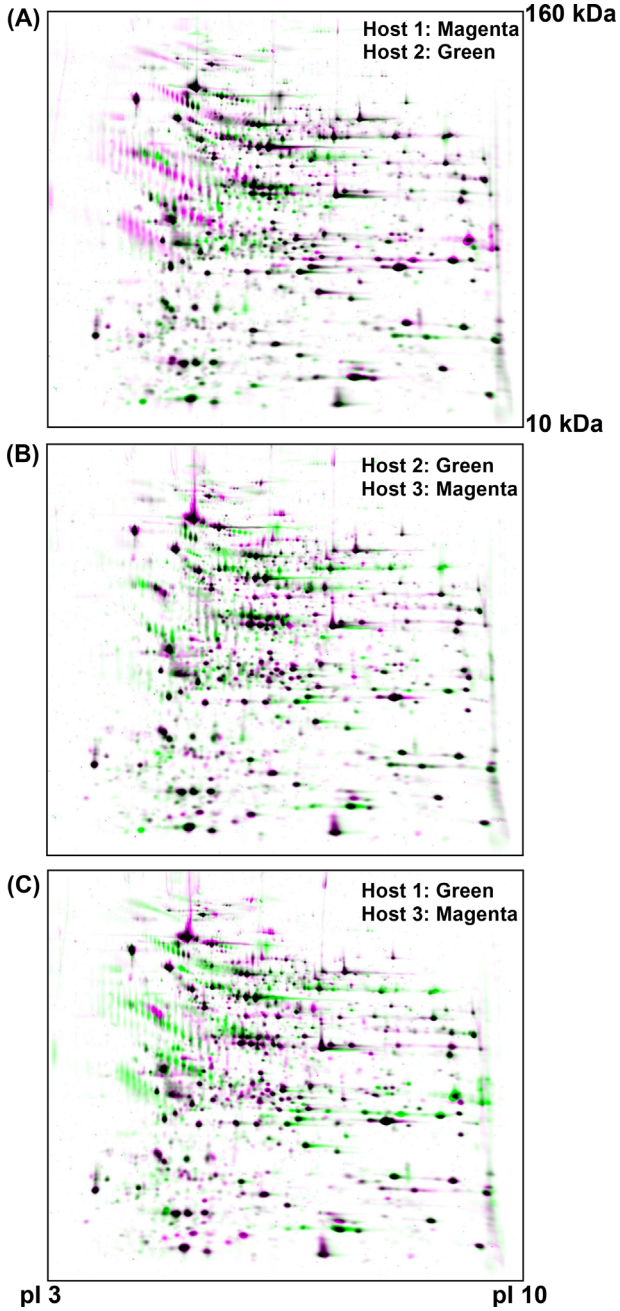

Figure 9. Pair-wise comparison of representative HCP patterns for three CHO cell lines by overlaying 2D-PAGE images for (**A**) Host 1 (magenta) and Host 2 (green), (**B**) Host 2 (green) and Host 3 (magenta), and (**C**) Host 1 (green) and Host 3 (magenta). Day 14 culture supernatants from null runs in 2 L bioreactors were stained with SYPRO Ruby. Each image represents an overlay of composite images from two cell lines. The composite image for each cell line was generated from six replicate gel images from duplicate bioreactors.

The apparent bias towards acidic proteins via 2D-PAGE analysis observed here (Figs. 8 and 9) was previously reported for CHO culture supernatant samples (Jin et al., 2010). This bias should include secreted proteins and intracellular proteins released by cell lysis. Since this acidic bias was not apparent in the CHO cell pellet samples previously analyzed (Krawitz et al., 2006), and a significant portion of the CHO-K1 proteome is glycosylated (Baycin-Hizal et al., 2012), we speculate that this bias reflects contributions from secreted proteins that are heavily glycosylated.

Ultimately, without further investigation, it is hard to discern if the 2D-PAGE spot patterns across Hosts 1–3 (Figs. 8 and 9) are more sensitive to cell line, upstream process, culture viability or other cell culture attributes. However, some of these spot differences are likely due to extracellular modifications. In a typical cell culture environment, extracellular proteins are subject to chemical modifications like deamidation (Zheng and Janis, 2006) and glycation (Yuk et al., 2011), to proteolytic degradation by proteases that are secreted or released upon cell lysis (Ryll et al., 2000; Yang and Butler, 2000), and to removal of post-translational modifications by glycosidases (Gramer and Goochee, 1993). The extent of these types of extracellular modifications should increase with culture duration, and should result in charge and/or size heterogeneity that can be detected by 2D-PAGE.

In addition, some of the 2D-PAGE spot differences may be due to intracellular processing. For example, NH_4^+, osmolality, or pCO_2 levels in CHO cultures can affect the glycosylation of recombinant and native proteins (Hossler et al., 2009; Pacis et al., 2011; Zanghi et al., 1999). Considering the differences in $NH4^+$, osmolality, and pCO_2 profiles in our null runs (Fig. 3), we may expect differences in glycosylation of secreted HCPs across Hosts 1–3 and also across culture duration within a cell line. We previously observed changes in both charge variant and glycosylation profiles over culture duration for an IgG1 produced by a recombinant cell line derived from the same CHO strain as Host 1 (Yuk et al., 2015). Likewise, our Genentech colleagues also observed changes in glycosylation profiles, correlating with increasing osmolality over culture duration, for several other recombinant IgG1s produced by cell lines derived from the same CHO strain as Host 1 (Pacis et al., 2011). By extension, secreted HCPs can also display these types of glycoform differences that may be captured by 2D-PAGE.

HCP Profiles by LC-MS/MS

In our previous work, to understand the reasons for differences observed in 2D-PAGE spot patterns of cell pellet samples from three null CHO cell lines, we excised the differentially expressed spots and identified them by MS (Krawitz et al., 2006). Our previous study revealed that only a small number of these spots were the result of apparent qualitative (on-off) differences, and that the differences were due to post-translational modifications or protein isoforms rather than bone fide on-off differences in protein expression. Our earlier findings are consistent with the limitations associated with

2D-PAGE (Chevalier 2010; Godovac-Zimmermann and Brown, 2001; Rabilloud et al., 2010), especially with respect to its use in HCP analysis (Tscheliessnig et al., 2013; Valente et al., 2014).

In this work, we utilized advances in label-free LC-MS/MS shotgun proteomics for detecting and quantifying differential protein expression (Zhang et al., 2006), and for identifying HCP species present at low levels in drug substance samples (Reisinger et al., 2014). Although two-dimensional liquid chromatography coupled to MS has also been proven effective for HCP analysis (Doneau et al., 2012; Schenauer et al., 2012; Zhang et al., 2014), we chose here to rely on the one-dimensional LC-MS/MS approach because it has higher throughput and is more robust (Reisinger et al., 2014).

In applying this orthogonal proteomics approach towards a semi-quantitative analysis of HCPs across Hosts 1–3, we found that the overall LC-MS/MS spectral and peptide counts were reproducible between technical replicates (data not shown), and that the numbers of peptides and proteins identified were comparable within biological replicates for each cell line and across cell lines (Table II). When we searched the LC-MS/MS data for the expression of our HCP of interest, we found that PLBL2 spectral counts differed significantly across Hosts 1–3 ($P < 0.01$) and correlated linearly with measurements by PLBL2 ELISA ($R^2 = 0.90$; $P < 0.01$).

A comparable number of peptides and proteins identified by LC-MS/MS (Table II) may not translate into comparable HCP populations. To explore this possibility, we compared the identities of the top 1,000 proteins identified by LC-MS/MS across Hosts 1–3 and found considerable overlap: 80% of the identified CHO proteins were common to supernatants from all three cell lines. Considering that the overlap in top 1,000 proteins achieved for technical replicates was 92–93%, the 80% overlap across Hosts 1–3 indicates that the overall protein populations were very similar amongst these different null CHO cell lines cultured in their respective upstream processes. These findings are consistent with our expectation that extracellular modifications and glycoform variations result in different spot patterns by 2D-PAGE, but they do not change the overall protein populations in the samples, as indicated by our LC-MS/MS findings. When Carlage et al. (2009) used LC-MS/MS to compare the proteomes of two recombinant cell lines derived from the same CHO DG44 host, they identified 339 proteins in the high producer, and 352 proteins in the low producer. Although they did not reveal the overlap in the identities of the proteins between the two CHO cell lines, they provided the number of proteins detected in six categories based on their cellular origins. If we assume that the overlap in the number of proteins within each category corresponded to a 100% match in protein identities, the number of proteins identified that were common to both the high and low producers would be 296. Therefore, the 80% overlap in the top 1,000 proteins detected across Hosts 1–3 is comparable to the theoretical maximum overlap of ~85% across two recombinant CHO DG44 cell lines (Carlage et al., 2009).

When we compared the HCP expression of Host 3 across run duration, the overlap was found to be 86% amongst the top 1,000 identified proteins observed across the three time-points (days 10, 14, and 17). This suggests that as culture viability drops, the predominant HCP population does not significantly change, and is consistent with the observation that PLBL2 was observed in HCCF at all cell culture viabilities tested in this study. Levy et al. (2014) also reported similar findings using supernatant from cultures harvested at 97–99% viability: two-thirds of the proteins that interact with recombinant antibody products were characterized as intracellular proteins. For Host 3, LC-MS/MS analysis showed no significant differences in the number of peptides ($P = 0.33$) or proteins ($P = 0.11$), or in the PLBL2 spectral counts ($P = 0.11$) for culture supernatants taken on days 10, 14, and 17. Likewise, we obtained comparable HCP levels for these Host 3 samples, as evaluated by HCP ELISA (Fig. 4A) and PLBL2 ELISA (Fig. 5A). In addition, the plateau in extracellular levels of immunogenic HCP and PLBL2 is reminiscent of the plateau in extracellular product titer sometimes observed for recombinant CHO cell lines, which also typically coincides with viability decline (Hsu et al., 2012; Yuk et al., 2015); these observations indicate that cellular protein production may stall when cells lose viability.

Conclusions

The three null cell lines tested here were similar in their cell-specific productivities for immunogenic HCPs, as well as in the total numbers and major populations of proteins detected in day 14 supernatants by LC-MS/MS (Table III). These findings are surprising, in light of the diversity in upstream inputs (Table I)—which ranged from differences in CHO lineage, adaptation history, upstream processes, and resulting cell culture performances (Figs. 2 and 3)—as well as the distinct protein spot patterns by 2D-PAGE (Fig. 9). The weight of the evidence indicates that switches amongst these cell lines (inexorably tied to their corresponding upstream processes) should not result in order-of-magnitude differences in the amount of immunogenic HCP, or in

Table II. Number of peptides and proteins identified as well as PLBL2 spectral counts obtained by LC-MS/MS analysis of culture supernatants from null runs with three CHO cell lines (Hosts 1–3).

Cell line (#biological replicates)	Day	#Peptides identified	#Proteins identified[a]	Normalized spectral counts for PLBL2
Host 1 ($n = 2$)	14	16532 ± 451	1483 ± 24	96 ± 6
Host 2 ($n = 3$)	14	15576 ± 1150	1439 ± 79	65 ± 15
Host 3 ($n = 3$)	14	16174 ± 560	1434 ± 53	49 ± 2
Host 3 ($n = 2$)	10	15432 ± 59	1350 ± 4	55 ± 2
Host 3 ($n = 2$)	17[b]	15535 ± 723	1363 ± 43	43 ± 7

[a]For the top 1,000 ranked proteins identified in day 14 samples, the overlap across Hosts 1–3 was 80%. For the top 1,000 ranked proteins identified in Host 3 samples, the overlap across days 10, 14, and 17 was 86%. For technical replicates, the overlap for a given sample was 92–93%.

[b]For Host 3, culture duration was extended to day 17 for two of the three replicate bioreactors.

Table III. Summary of HCP analyses for Hosts 1-3.

HCP Analysis	Details	Host 1	Host 2	Host 3
ELISA	Q_{HCP}[a]	2.8	2.6	2.9
2D-PAGE	Overlay of images[b]	Qualitative differences observed by pairwise comparison		
LC-MS/MS	#Proteins identified[c]	1483 ± 24	1439 ± 79	1434 ± 53
LC-MS/MS	Overlap in proteins[c]	80% overlap in top 1,000 ranked proteins identified in day 14 samples		

[a]Refer to Figure 4C. Q_{HCP} values were estimated from the linear regression of HCP concentration in supernatant versus vol.IVPCV and represented here in units of g per L of viable cells per day. Q_{HCP} values were not statistically different across Hosts 1–3 ($P = 0.87$ by ANCOVA).

[b]Refer to Figure 9.

[c]Refer to Table II. The overlap in top 1,000 ranked proteins identified in technical replicates was 92–93%.

the number and identities of the HCPs present in the feedstock for downstream processing. When we applied these HCP analyses to supernatant samples from the cell line (Host 3) that showed a sharp drop in viability after day 10, we observed no significant changes in the amounts of immunogenic HCP and PLBL2, or in the numbers and major species of HCPs detected across days 10, 14, and 17, despite multifold increases in extracellular LDH levels. The Host 3 findings provide a counter example in which a delay to the harvest operation upon viability decline may not affect the amount and composition of HCPs in the feedstock for downstream processing as severely as originally expected. In addition, despite the higher viabilities (>70%) observed for Host 1 and 2 cultures, their extracellular LDH levels at day 14 were comparable to that of Host 3 cultures with low final viabilities (<25%). These LDH findings demonstrate that the cumulative extent of cell lysis in high cell density ($>10^7$ cells/mL) CHO cultures can be considerable. Therefore, cell lysis in these fed-batch cultures would contribute to the extracellular presence of intracellular HCPs such as PLBL2.

We thank Analytical Operations, especially Benjamin Ou, Margaret Lin, Sara Parker, and Zoe Kuznia, for performing HCP, ELISA, and LDH assays; Andrew Hu and Jacob B. Mauger for technical assistance with the 2 L bioreactor runs; Kathy Francissen and Robert Ming Wong for helpful discussions; and John Joly, John Stults, Bob Kiss, Andy Lin, and Pat Rancatore for supporting this cross-functional collaboration.

Nomenclature

2D-PAGE	two-dimensional polyacrylamide gel electrophoresis
2-D DIGE	two-dimensional fluorescence difference gel electrophoresis
%PCV	percent packed cell volume
ANOVA	one-way analysis of variance
ANCOVA	analysis of covariance, unequal slopes
CHO	Chinese hamster ovary
ELISA	enzyme-linked immunosorbent assay
HCP	host cell protein
IVPCV	integrated viable packed cell volume
LC-MS/MS	liquid chromatography coupled with tandem mass spectrometry
LDH	lactate dehydrogenase
MS	mass spectrometry
MS/MS	tandem mass spectrometry
n	number of biological replicates
pCO_2	carbon dioxide partial pressure
PCV	packed cell volume
PLBL2	phospholipase B-like 2
Q_{HCP}	cell-specific productivity with respect to HCP
Q_{PLBL2}	cell-specific productivity with respect to PLBL2
R^2	correlation of determination
V	viability
VCD	viable cell density
vol.IVPCV	volumetric integrated viable packed cell volume
vol.PCV	volumetric packed cell volume
WCCF	whole cell culture fluid

References

Bayzin-Hizal D, Tabb DL, Chaerkady R, Chen L, Lewis NE, Nagarajan H, Sarkaria V, Kumar A, Wolozny D, Colao J, Jacobson E, Tian Y, O'Meally RN, Krag SS, Cole RN, Palsson BO, Zhang H, Betenbaugh M. 2012. Proteomic analysis of Chinese hamster ovary cells. J Proteome Res 11:5265–5276.

Carlage T, Hincapie M, Zang L, Lyubarskaya Y, Madden H, Mhatre R, Hancock WS. 2009. Proteomic profiling of a high-producing Chinese hamster ovary cell culture. Anal Chem 81:7357–7362.

Champion KM, Nishihara JC, Joly JC, Arnott D. 2001. Similarity of the *Escherichia coli* proteome upon completion of different biopharmaceutical fermentation processes. Proteomics 1:1133–1148.

Chapra SC, Canale RP. 1988. Numerical methods for engineers, 2nd ed. New York: McGraw-Hill.

Chevalier F. 2010. Highlights on the capacities of "Gel-based" proteomics. Proteome Sci 8:23.

Doneau CE, Xenopoulos A, Fadgen K, Murphy J, Skilton SJ, Prentice H, Stapels M, Chen W. 2012. Analysis of host-cell proteins in biotherapeutic proteins by comprehensive online two-dimensional liquid chromatography/mass spectrometry. mAbs 4:24–44.

Godovac-Zimmermann J. Brown LR. 2001. Perspectives for mass spectrometry and functional proteomics. Mass Spectrom Rev 20:1–57.

Gramer MJ, Goochee CF. 1993. Glycosidase activities in Chinese hamster ovary cell lysate and cell culture supernatant. Biotechnol Prog 9:366–373.

Grzeskowiak JK, Tscheliessnig A, Toh PC, Chusainow J, Lee YY, Wong N, Jungbauer A. 2009. 2-D DIGE to expedite downstream process development for human monoclonal antibody purification. Protein Expr Purif 66:58–65.

Hossler P, Khattak SF, Li ZJ. 2009. Optimal and consistent glycosylation in mammalian cell culture. Glycobiology 19:936–949.

Hsu W-T., Aulakh RPS, Traul DL, Yuk IH. 2012. Advanced microscale bioreactor system: A representative scale-down model for bench-top bioreactors. Cytotechnology 64:667–678.

Hu Z, Guo D, Yip SSM, Zhan D, Misaghi S, Joly JC, Snedecor BR, Shen AY. 2013. Chinese hamster ovary (CHO) K1 host cell enables stable cell line development for antibody molecules which are difficult to express in DUXB11-derived dihydrofolate reductase (DHFR) deficient host cell. Biotechnol Prog 29:980–985.

Jensen AG, Chemali M, Chapel A, Kieffer-Jaquinod S, Jadot M, Garin J, Journet A. 2007. Biochemical characterization and lysosomal localization of the mannose-6-phosphate protein p76 (hypothetical protein LOC196463). Biochem J 402:449–458.

Jin M, Szapiel N, Zhang J, Hickey H, Ghose S. 2010. Profiling of host cell proteins by two-dimensional gel electrophoresis (2D-DIGE): Implications for downstream process development. Biotechnol Bioeng 105:306–316.

Kao F-T., Puck TT. 1968. Genetics of somatic mammalian cells, VII. Induction and isolation of nutritional mutants in Chinese hamster cells. Proc Natl Acad Sci USA 60:1275–1281.

Krawitz DC, Forrest W, Moreno GT, Kittleson J, Champion KM. 2006. Proteomic studies support the use of multi-product immunoassays to monitor host cell protein impurities. Proteomics 6:94–110.

Lakomek K, Dickmanns A, Kettwig M, Urlaub H, Ficner R, Lubke T. 2009. Initial insight into the function of the lysosomal 66.3kDa protein from mouse by means of X-ray crystallography. BMC Struct Biol 9:56.

Levy NE, Valente KN, Choe LH, Lee KH, Lenhoff AM. 2014. Identification and characterization of host cell protein product-associated impurities in monoclonal antibody bioprocessing. Biotechnol Bioeng 111:904–912.

Lewis NE, Liu X, Li Y, Nagarajan H, Yerganian G, O'Brien E, Bordbar A, Roth AM, Rosenbloom J, Bian C, Xie M, Chen W, Li N, Baycin-Hizal D, Latif H, Forster J, Betenbaugh MJ, Famili I, Xu X, Wang J, Palsson BO. 2013. Genomic landscapes of Chinese hamster ovary cell lines as revealed by the *Cricetulus griseus* draft genome. Nat Biotechnol 31:759–765.

McDonald P, Victa C, Carter-Franklin JN, Fahrner R. 2009. Selective antibody precipitation using polyelectrolytes: A novel approach to the purification of monoclonal antibodies. Biotechnol Bioeng 102:1141–1151.

Nishihara JC, Champion KM. 2002. Quantitative evaluation of proteins in one- and two-dimensional polyacrylamide gels using a fluorescent stain. Electrophoresis 23:2203–2215.

Omasa T, Higashiyama K, Shioya S, Suga K. 1992. Effects of lactate concentration on hybridoma culture in lactate-controlled fed-batch operation. Biotechnol Bioeng 39:556–564.

Pacis E, Yu M, Autsen J, Bayer R, Li F. 2011. Effects of cell culture conditions on antibody N-linked glycosylation—what affects high mannose 5 glycoform. Biotechnol Bioeng 108:2348–2358.

Petersen JF, McIntire LV, Papoutsakis ET. 1988. Shear sensitivity of cultured hybridoma cells (CRL-8018) depends on mode of growth, culture age and metabolite concentration. J Biotechnol 7:229–246.

Puck TT, Cieciura SJ, Robinson A. 1958. Genetics of somatic mammalian cells. III. Long-term cultivation of euploid cells from human and animal subjects. J Exp Med 108:945–956.

Rabilloud T, Chevallet M, Luche S, Lelong C. 2010. Two-dimensional gel electrophoresis in proteomics: Past, present, and future. J Proteomics 73:2064–2077.

Racher AJ, Looby D, Griffiths JB. 1990. Use of lactate dehydrogenase release to assess changes in culture viability. Cytotechnology 3:301–307.

Reisinger V, Toll H, Mayer RE, Visser J, Wolschin F. 2014. A mass spectrometry-based approach to host cell protein identification and its application in a comparability exercise. Anal Biochem 463:1–6.

Ryll T, Dutina G, Reyes A, Gunson J, Krummen L, Etcheverry T. 2000. Performance of small-scale CHO perfusion cultures using an acoustic cell filtration device for cell retention: Characterization of separation efficiency and impact of perfusion on product quality. Biotechnol Bioeng 69:440–449.

Schenauer MR, Flynn GC, Goetze AM. 2012. Identification and quantification of host cell protein impurities in biotherapeutics using mass spectrometry. Anal Biochem 428:150–157.

Shukla AA, Jiang C, Ma J, Rubacha M, Flansburg L, Lee SS. 2008. Demonstration of robust host cell protein clearance in biopharmaceutical downstream processes. Biotechnol Prog 24:615–622.

Singh SK. 2011. Impact of product-related factors on immunogenicity of biotherapeutics. J Pharm Sci 100:354–387.

Tait AS, Hogwood CEM, Smales CM, Bracewell DG. 2012. Host cell protein dynamics in the supernatant of a mAb producing CHO cell line. Biotechnol Bioeng 109:971–982.

Tscheliessnig AL, Konrath J, Bates R, Jungbauer A. 2013. Host cell protein analysis in therapeutic protein bioprocessing—methods and applications. Biotechnol J 8:655–670.

Urlaub G, Chasin LA. 1980. Isolation of Chinese hamster cell mutants deficient in dihydrofolate reductase activity. Proc Natl Acad Sci USA 77:4216–4220.

Valente KN, Schaefer AK, Kempton HR, Lenhoff AM, Lee KH. 2014. Recovery of Chinese hamster ovary host cell proteins for proteomic analysis. Biotechnol J 9:87–99.

Valente KN, Lenhoff AM, Lee KH. 2015. Expression of difficult-to-remove host cell protein impurities during extended Chinese hamster ovary cell culture and their impact on continuous bioprocessing. Biotechnol Bioeng 10.1002/bit.25515.

Vanderlaan M, Sandoval W, Liu P, Nishihara J, Tsui G, Lin M, Parker S, Wong RM, Low J, Wang X, Yang J, Veeravalli K, McKay P, O'Connell L, Tran B, Vij R, Fong C, Francissen F, Zhu-Shimoni J, Quarmby V, Krawitz D. 2015. Hamster Phospholipase B-like 2 (PLBL2), a host cell protein impurity in CHO-derived therapeutic monoclonal antibodies. BioProcess Int 13:18–29.

Wang X, Hunter AK, Mozier NM. 2009. Host cell proteins in biologics development: Identification, quantitation and risk assessment. Biotechnol Bioeng 103:446–458.

Yang M, Butler M. 2000. Enhanced erythropoietin heterogeneity in a CHO culture is caused by proteolytic degradation and can be eliminated by a high glutamine level. Cytotechnology 34:83–99.

Yu XC, Joe K, Zhang Y, Adriano A, Wang Y, Gazzano-Santoro H, Keck RG, Deperalta G, Ling V. 2011. Accurate determination of succinimide degradation products using high fidelity trypsin digestion peptide map analysis. Anal Chem 83: 5912–5919.

Yuk IH, Zhang B, Yang Y, Dutina G, Leach KD, Vijayasankaran N, Shen AY, Andersen DC, Snedecor BR, Joly JC. 2011. Controlling glycation of recombinant antibody in fed-batch cell cultures. Biotechnol Bioeng 108:2600–2610.

Yuk IH, Russell S, Tang Y, Hsu W-T., Mauger JB, Aulakh RPS, Luo J, Gawlitzek M, Joly JC. 2015. Effects of copper on CHO cells: Cellular requirements and product quality considerations. Biotechnol Prog 31:226–238.

Zanghi JA, Schmelzer AE, Mendoza TP, Knop RH, Miller WM. 1999. Bicarbonate concentration and osmolality are key determinants in the inhibition of CHO cell polysialylation under elevated pCO_2 or pH. Biotechnol Bioeng 65:182–191.

Zeid J, Harinarayan C, van Reis R. 2009. The impact of protein exclusion on the purity performance of ion exchange resins. Biotechnol Bioeng 102:971–976.

Zhang B, VerBerkmoes NC, Langston MA, Uberbacher E, Hettich RL, Samatova NF. 2006. Detecting differential and correlated protein expression in label-free shotgun proteomics. J Proteome Res 5:2909–2918.

Zhang Q, Goetze AM, Cui H, Wylie J, Trimble S, Hewig A, Flynn GC. 2014. Comprehensive tracking of host cell proteins during monoclonal antibody purifications using mass spectrometry. MAbs 6:659–670.

Zheng JY, Janis LJ. 2006. Influence of pH, buffer species, and storage temperature on physicochemical stability of a humanized monoclonal antibody LA298. Int J Pharm 308:46–51.

Zhu MM, Goyal A, Rank DL, Gupta SK, Vanden Boom T, Lee SS. 2005. Effects of elevated pCO_2 and osmolality on growth of CHO cells and production of antibody-fusion protein B1: A case study. Biotechnol Prog 21:70–77.

Zhu-Shimoni J, Yu C, Nishihara J, Wong RM, Gunawan F, Lin M, Krawitz D, Liu P, Sandoval W, Vanderlaan M. 2014. Host cell protein testing by ELISAs and the use of orthogonal methods. Biotechnol Bioeng 111:2367–2379.